Journal of the Korean Ceramic Society
Vol. 43, No. 3, pp. 143~147, 2006.

Nano-Granular Co-Fe-Al-O Soft Ferromagnetic Thin Films for GHz Magnetic Device Applications

Jae Cheon Sohn† and Dongjin Byun*

Future Technology Research Division, Korea Institute of Science and Technology, Seoul 130-650, Korea
**Department of Materials Science and Engineering, Korea University, Seoul 136-701, Korea*
(Received November 10, 2005; Accepted November 29, 2005)

ABSTRACT

Co-Fe-Al-O nanogranular thin films were fabricated by RF-magnetron sputtering under an $Ar+O_2$ atmosphere. High resolution transmission electron microscopy revealed that the Co-Fe-Al-O films are composed of bcc (Co, Fe) nanograins finer than 5 nm and an Al-O amorphous phase. A very large electrical resistivity of 374 μΩcm was obtained, together with a large uniaxial anisotropy field of 50 Oe, a hard axis coercivity of 1.25 Oe, and a saturation magnetization of 12.9 kG. The actual part of the relative permeability was measured to be 260 at low frequencies and this value was maintained up to 1.3 GHz. The ferromagnetic resonance frequency was 2.24 GHz. The resulting Co-Fe-Al-O nanogranular thin films with a high electrical resistivity and high resonance frequency are considered to be suitable for GHz magnetic device applications.

Key words **: *Nano-granular thin film, Soft ferromagnetic, Ferromagnetic resonance***

1. Introduction

With a large volume of information and a variety of communication media such as mobile telephones and satellite broadcasting devices, the development of high-frequency devices is of significant practical importance. The goal of mobile/wireless communications in the coming years will be to allow users to access the global network at any time, without regard to mobility or location. Continuing developments in satellite communications, fiber-optic and digital microwave radio communications are aimed at this goal. Many component devices such as band-pass filters, duplexers and resonators must also conform to high-frequency bands.[1,2]

As the operating frequency of the Radio Frequency (RF) wireless communication devices is usually very high being in the GHz range, the magnetic materials utilized in them should exhibit a high FMR frequency (f_R). A high f_R can be obtained at a large saturation magnetization ($4\pi M_s$) and anisotropy field (H_K), according to the equation $f_R=(\gamma/2\pi)(4\pi M_S H_K)^{1/2}$ obtained for a single domain magnetic thin film. Here γ is the gyromagnetic ratio. Another important requirement is a high electrical resistivity (ρ); otherwise, the eddy current losses are extremely large in the GHz frequency range. Of course, a high relative permeability (μ_r) is desirable, since μ_r is directly related with the level of the output signals of the RF magnetic devices. In the case of bulk ferrites with a small $4\pi M_s$ value, μ_r is low and f_R is also relatively low. This is the reason why bulk ferrites are not widely used in high-frequency applications, although they are mostly insulators. On the other hand, ferromagnetic metals generally have a large μ_r value due to their large $4\pi M_s$ value and relatively small H_K value. However, the main limiting factor is a small ρ value, causing large eddy current losses. Thus, ferromagnetic metals are not suitable for practical use in the high frequency region. Consequently, magnetic materials suitable for high-frequency RF applications should have a large $4\pi M_s$ value and a high H_K value, thereby increasing f_R, as well as a large ρ value, thereby reducing eddy current losses.[3-5]

Recently developed nano-granular magnetic thin films were known to meet these requirements. The nano-granular thin films consist of nano-meter scale ferromagnetic grains and these grains are usually completely separated by an insulating phase such as an oxide, nitride, or boride. This microstructural feature is important to achieve a high ρ value. Exchange coupling between nano-granules still exists across the insulating boundary. This is a necessary condition for the random anisotropy model by which the effective magnetocrystalline anisotropy is greatly reduced, resulting in excellent magnetic softness.[6] Thus, it is expected that the nano-granular magnetic thin films have a high μ_r value and low eddy current losses even in the high frequency region.

Previous work on Fe-based nano-granular magnetic thin films has shown a relatively high $4\pi M_s$, value but small H_K. This is insufficient for high frequency operation, as the resulting f_R is not high enough for GHz-level frequency applications.[7-9] On the other hand, Co-based magnetic thin

†Corresponding author : Jae Cheon Sohn
E-mail : jcsohn@kist.re.kr
Tel : +82-2-958-5427 Fax : +82-2-958-6851

films show a small μ_r value due to a relatively small $4\pi M_s$ value and large H_K value when compared to Fe-based magnetic thin films.[10,11] Co-Fe-based nanogranular alloys have combined merits of respective Fe- and Co-based alloys. The microstructural feature in which Co-Fe grains are completely surrounded with an insulating phase is essential to the realization of a high ρ value. Co-Fe-Al-O thin films with (Co, Fe) nanograins in an amorphous Al-O oxide matrix were reported to show very good soft magnetic properties even in the GHz range.[12] The thin films also exhibit a small coercivity, mainly due to a very small (nano-crystalline) (Co, Fe) grain size. Common applications of these thin films are inductors and noise suppressors in the GHz range. In these applications, a large magnetostriction is harmful in general and, accordingly, an alloy with a small magnetostriction was sought mainly by adjusting the Fe/Co ratio. A good magnetic softness and a high f_R value are the two key factors for the RF magnetic device applications. With this in mind, high-frequency soft magnetic properties of nanogranular Co-Fe-Al-O thin films are investigated in this work.

2. Experimental Procedure

Co-Fe-Al-O nanogranular thin films with a thickness of approximately 0.1 μm were fabricated by RF magnetron sputtering in an O_2 + Ar atmosphere. The background pressure was higher than 7×10^{-7} Torr. The O_2 flow ratio was varied mainly to a change in the oxygen content of the thin films. Co-Fe-Al composite targets composed of a Co-Fe alloy target and Al chips were used. The films were grown on Si substrates in a static field of 1 kOe to induce uniaxial magnetic anisotropy. The microstructure was examined by X-Ray Diffraction (XRD) using Cu$K\alpha$ radiation and by High-Resolution Transmission Electron Microscopy (HRTEM) combined with nano-beam electron diffraction. The overall composition of the films was determined by Electron Probe Microanalysis (EPMA) and Auger Electron Spectroscopy (AES). The composition of nanograins was mainly measured by Energy Dispersive X-ray spectroscopy (EDX) combined with HRTEM with a beam diameter of 2 nm. Magnetic properties were evaluated with a Vibrating Sample Magnetometer (VSM). The magnitude of f_R was obtained from the frequency profile of complex permeability, $\mu_r = \mu_r' + j\mu_r''$, measured up to 9 GHz with a pick-up coil-type permeameter. The value of ρ was obtained through using the conventional four-point probe method.

3. Results and Discussion

3.1. Microstructure

XRD patterns of as-deposited Co-Fe-Al-O films at various O_2 flow ratios are shown in Fig. 1. The input power (200 W) and the sputtering pressure (5 mTorr) were fixed, but the O_2 flow ratio is varied from 6.63 to 16.67%, as indicated in the figure. Also indicated is the grain diameter (d), which

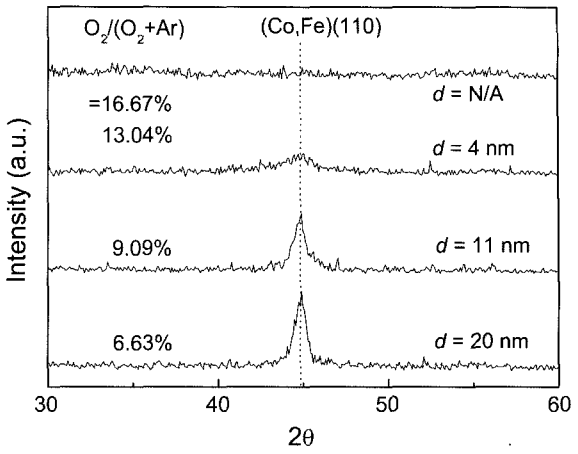

Fig. 1. XRD patterns of the as-deposited Co-Fe-Al-O films. The input power (200 W) and the sputtering pressure (5 mTorr) were fixed, but the O_2 flow ratio varied from 6.63 to 16.67% and indicated in the figure. Also indicated is the grain diameter (d), which was determined by using the Scherrer formula.

was determined by using the Scherrer formula. The (110) diffraction peak corresponding to the bcc (Co, Fe) phase was observed at low O_2 flow ratios of 6.63, 9.09 and 13.04%, but was absent at the highest O_2 flow ratio of 16.67%. No peaks related with oxides were observed, indicating that Al-O was present as an amorphous phase and (Co, Fe) grains were not oxidized, at least at a substantial amount to be detected by XRD. The absence of the bcc (Co, Fe) phase at the highest O_2 flow ratio may indicate that the amount of the bcc (Co, Fe) phase is significantly reduced at this high O_2 flow ratio. The width of the (110) peak increased and the height decreased with an increasing O_2 flow ratio, indicating a smaller grain size at a higher O_2 flow ratio. The reduction of the grain size with the increase of the O_2 flow ratio is in agreement with a previous observation,[14] as the amorphous Al-O phase surrounding (Co, Fe) grains provides a barrier for the diffusion of Co and Fe ions, thereby suppressing the crystal growth of the Co-Fe alloy grains.[15]

Fig. 2(a) through (h) show TEM micrographs and Selected Area electron Diffraction (SAD) patterns of the as-deposited Co-Fe-Al-O thin films prepared at two different O_2 flow ratios of 6.63% (Sample A) and 13.04% (Sample B). The compositions of nanograins of Sample A and B are those corresponding to $Co_{43}Fe_{40}Al_{15}O_2$ and $Co_{41}Fe_{38}Al_{13}O_8$ (in atomic %), respectively. It is seen from the planar TEM micrograph in Fig. 2(b) for Sample A that the microstructure is composed of large granules (dark dots) with a size of nearly 20 nm in an amorphous Al-O matrix (grey area). The cross-sectional TEM micrograph in Fig. 2(a) clearly shows a columnar growth of the granules. A clearer image of the (Co, Fe) grains can be seen from the planar high resolution TEM micrograph shown in Fig. 2(c). The value of r is somewhat low (57 μΩcm) for Sample A, indicating that the (Co, Fe) grains are not completely isolated from the amorphous Al-O matrix. Rather, these grains are

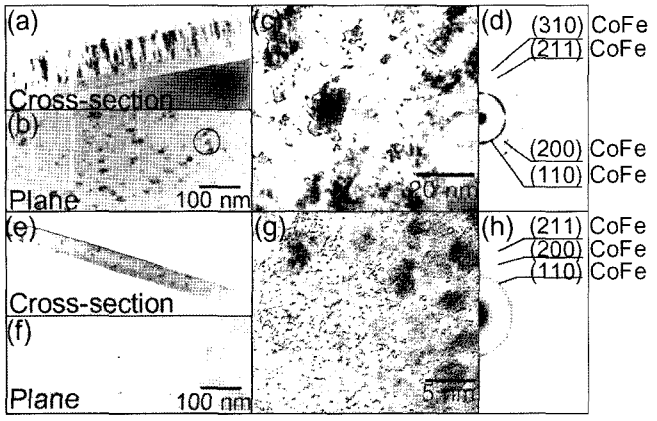

Fig. 2. TEM micrographs and SAD patterns are shown in (a) through (h). The results of as-deposited Co-Fe-Al-O films prepared at O_2 flow ratios of 6.63% (Sample A) and 13.04% (Sample B) are shown in (a) through (d), and (e) through (h), respectively.

interconnected, although this is not clear from the TEM micrographs. The increase of the oxygen content caused a severe change in the microstructure. The size of (Co, Fe) grains was much reduced, being 3~5 nm, and no columnar growth occurred. The value of ρ for Sample B was very high (374 μΩcm), indicating that each (Co, Fe) grain in this case was mostly isolated by the insulating Al-O amorphous phase. The HRTEM micrograph shown in Fig. 2(g) clearly shows this microstructural feature. SAD patterns are shown in Fig. 2(d) and (h) for Sample A and B, respectively. The diffraction rings of the SAD patterns are consistent with those expected from the bcc (Co, Fe) phase. It is interesting to note that the SAD patterns of Sample A with the lower oxygen content (Fig. 2(d)) are sharper than those of Sample B (Fig. 2(h)). No SAD patterns related with oxide phases were observed, in agreement with the XRD results.

3.2. Electrical Resistivity and Magnetic Properties

Fig. 3(a) shows the results for r in as-deposited Co-Fe-Al-O granular films as a function of the O_2 flow ratio at various input powers of 100, 200, and 300 W, but at a fixed sputtering pressure of 5 mTorr. For a given O_2 flow ratio, ρ increases with a decreasing input power, while at a given input power, it increases with an increasing O_2 flow ratio. This difference in ρ depending on the input power may be explained by the thermalization process. A sputtered light metal element, Al in this study, is considered to be highly thermalized in a high input power and is subjected to a high scattering, resulting in a low deposition rate.[16] As the input power increases, the amount of Al decreases, causing a low content of the Al-O phase. An abrupt increase in ρ occurs near an O_2 flow ratio of 20% in the cases of 200 W and 300 W. A possible reason for this is that the conductive path collapses near the O_2 flow ratio due to the percolation of the non-metallic, amorphous Al-O network.[17]

The O_2 flow ratio dependence of $4\pi M_s$, H_K, and coercivity (H_c) is shown in Fig. 3(b) for as-deposited Co-Fe-Al-O films

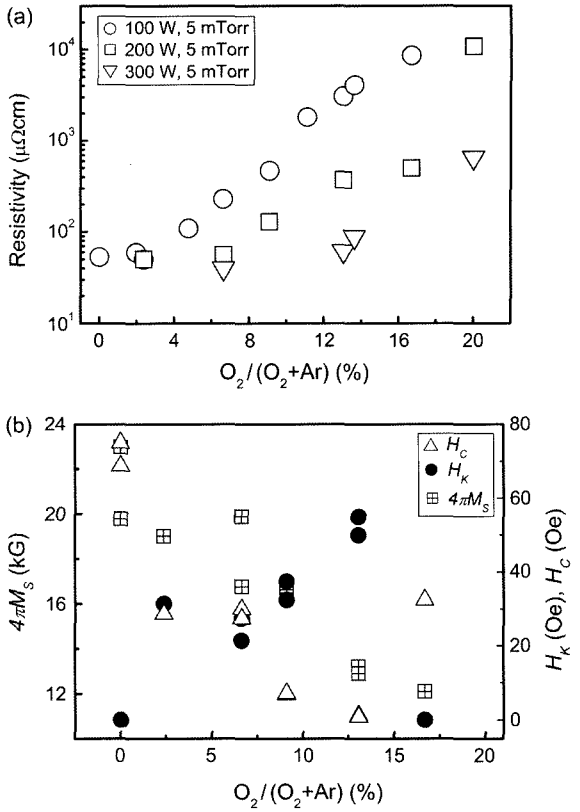

Fig. 3. (a) the magnitude of ρ of the as-deposited Co-Fe-Al-O films as a function of the O_2 flow ratio at various input powers of 100, 200, and 300 W, but at a fixed sputtering pressure of 5 mTorr and (b) the values of $4\pi M_S$, H_K, and H_c of as-deposited Co-Fe-Al-O films as a function of the O_2 flow ratio. The input power (200 W) and sputtering pressure (5 mTorr) were fixed.

fabricated at an input power of 200 W and a sputtering pressure of 5 mTorr. As the O_2 flow ratio increases from 0 to 16.67%, the value of $4\pi M_s$ decreases monotonically from 23 to 11.9 kG, while the value of H_K increases from 0 to 55 Oe and then decreases again to 0 Oe at the highest O_2 flow ratio of 16.67%. H_c tends to decrease with an increasing O_2 flow ratio and shows a minimum at an O_2 flow ratio of 13.04%. It is noted here that the values of $4\pi M_s$ and ρ for Sample B are 12.9 kG and 374 μΩcm, respectively, a suitably high $4\pi M_s$ being combined with a high ρ. The degradation of $4\pi M_s$ with the increased O_2 flow ratio is caused possibly by the formation of a non-magnetic phase at the outer region of the Co-Fe grains. This means that the oxidizing process takes place not only in the grain boundary but also in the grain itself. The decrease in H_C at the O_2 flow ratios of 13.04% and below is due to the nanocrystallization of Co-Fe alloy grains. In the well-known random anisotropy model for nanocrystalline soft magnetic materials,[18] H_C is proportional to the sixth power of the grain size. It is important to note that H_C rapidly increases at O_2 flow ratios above 13.04%, possibly due to a weak exchange coupling between ferromagnetic grains across a very thick non-magnetic Al-O amorphous phase. It is further noteworthy that, in the random

anisotropy model, exchange coupling among magnetic grains is essential for a reduction of the effective magneto-crystalline anisotropy.[18]

As was mentioned previously, the following relationship exists among f_R, $4\pi M_S$, and H_K; $f_R = (\gamma/2\pi)(4\pi M_S H_K)^{1/2}$. $4\pi M_s$ and H_K are two important factors for f_R. In this study, the films were deposited in a static field as high as 1 kOe to induce a large uniaxial anisotropy. A static field of 1 kOe during sputtering, which was made possible with a specially designed sample holder, is considered to be high enough to completely saturate the sample, as this magnitude of applied field is much larger than the coercivity of the samples. However, induced anisotropy is not always formed; for example, at a fixed sputtering pressure of 5 mTorr, the induced anisotropy is not formed at input powers of 100 and 300 W, but is formed at an intermediate input power of 200 W. Although the precise reason for this is not clearly understood at this point, it seems somehow related to the microstructure. A detailed microstructural investigation shows that nanocrystalline grains with a grain size smaller than approximately 5 nm are observed only at an input power of 200 W (and also at a suitable oxygen flow ratio). Pair ordering is known to be the reason for the induced anisotropy. This means that atomic diffusion should occur during the deposition in order for the induced anisotropy to be formed. In general, atomic diffusion in bulk crystals is (much) lower than that in the amorphous phase or grain boundary. This mainly explains the well-known fact that the induced anisotropy is more easily formed; moreover, its magnitude is generally larger in amorphous materials. The large induced anisotropy observed in this study for thin films with ultra-small grains can similarly be explained. With nano-crystalline grains whose grain size is in the range of 5 nm, there is a significant portion of grain boundary, resulting in enhanced atomic diffusion. In Fig. 3(b), considering the relationship between the H_K and the O_2 flow ratio, the induced anisotropy reaches a maximum value at 13.03% and then suddenly decreases above 13.03%.

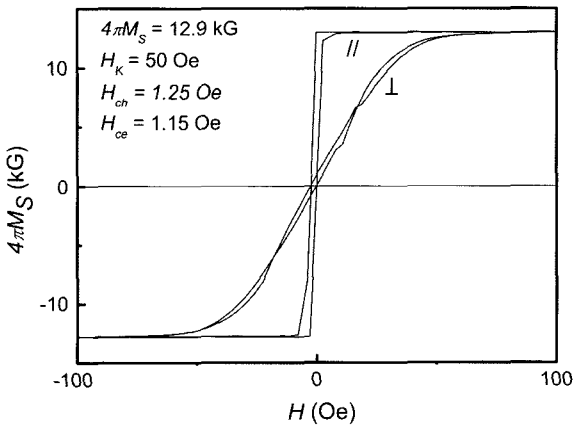

Fig. 4. Hysteresis loops of Sample B, measured under in-plane fields applied in the directions parallel and perpendicular to the induced anisotropy.

Hysteresis loops of Sample B, measured under in-plane fields in the directions parallel and perpendicular to the induced anisotropy, are shown in Fig. 4. Important magnetic properties are; $4\pi M_S = 12.9$ kG, $H_K = 50$ Oe, H_{ch} (in the perpendicular, difficult direction) = 1.25 Oe, and H_{ce} (in the parallel, easy direction) = 1.15 Oe. The thin film indeed exhibits a very good magnetic softness, combined with the high values of $4\pi M_S$ and H_K, which are important parameters for f_R.

The real and imaginary parts of the effective permeability for Sample B are measured in the very high frequency range, up to 9 GHz. The results are described in great detail in another work.[19] The actual part of the permeability (μ') is nearly flat up to 1 GHz and, in this frequency range, the imaginary part of the permeability is very low. The imaginary part (μ'') shows a peak at f_R (= 2.24 GHz). The measured value of the (pseudo) dc permeability is 260. The theoretical permeability spectra are computed by using the Landau-Lifshitz-Gilbert equation. The agreement between the experimental and theoretical results is workable in most cases. The calculated value of the (pseudo) dc permeability is 258 based on the rotation magnetization mechanism, and this value is in excellent agreement with the measured value of 260. This agreement indicates that the magnetization mainly occurs by spin rotation.

4. Conclusions

Co-Fe-Al-O nanogranular films with excellent soft magnetic properties at high frequencies were fabricated by RF magnetron reactive sputtering. A systematic investigation concerning the microstructure, electrical, and magnetic properties indicates a large role by the oxygen content in the thin films. Important electrical and magnetic properties of a typical thin film with the composition (in atomic %) $Co_{41}Fe_{38}Al_{13}O_8$ are; 374 μΩcm (ρ), 12.9 kG ($4\pi M_S$), 50 Oe (H_K), 1.25 Oe (H_{ce}), and 1.15 Oe (H_{ch}), 260 (μ') and 2.24 GHz (f_R).

REFERENCES

1. K. H. Kim, M. Yamaguchi, K. I. Arai, H. Nagura, and S. Ohnuma, "Effect of Radio-Frequency Noise Suppression on the Coplanar Transmission Line Using Soft Magnetic Thin Film," *J. Appl. Phys.*, **93** [10] 8002-04 (2003).
2. K. H. Kim, M. Yamaguchi, S. Ikeda, and K. I. Arai, "Modeling for RF Noise Suppressor Using a Magnetic Film on Coplanar Transmission Line," *IEEE Trans. Magn.*, **39** [5] 3031-33 (2003).
3. M. Fujimoto, "Inner-Stress Induced by Cu Metal Precipitation at Grain Boundaries in Low Temperature Fired Ni-Zn-Cu Ferrite," *J. Am. Ceram. Soc.*, **77** 2873-78 (1994).
4. M. Fujimoto, "Cu Multiply Twinned Particle Precipitation in Low Temperature Fired Ni-Zn-Cu Ferrite," *Jpn. J. Appl. Phys.*, **32** 5532-36 (1993).
5. M. Fujimoto, T. Suzuki, Y. Nishi, K. Arai, and S. Sekiguchi,

"Coherent Precipitation of Metal Copper in Low-Temperature-Fired Ni-Zn-Cu Ferrite," *J. Am. Ceram. Soc.*, **81** [9] 2477-80 (1998).

6. M. Yamaguchi, K. Suezawa, K. I. Arai, Y. Takahasi, S. Kikuchi, Y. Shimada, W. D. Li, S. Tanabe, and K. Ito, "Microfabrication and Characteristic of Magnetic Thin-Film Inductors in the Ultra High Frequency Region," *J. Appl. Phys.*, **85** 7919-22 (1999).
7. J. Y. Park, S. R. Kim, J. Kim, K. Y. Kim, S. H. Han, and H. J. Kim, "Soft Magnetic Properties and Microstructures of As-Sputtered Fe-M-O (M = Hf, Al) Films," *J. Magn. Soc. Jpn.*, **23** [1-2] 243-45 (1999).
8. H. J. Lee, S. Mitani, T. Shima, S. Nagata, and H. Fujimori, "Soft Magnetic Properties and Electrical Resistivity of Fe-Mg-O Thin Films Sputter-Deposited on Cooled Substrates," *J. Magn. Soc. Jpn.*, **23** [1-2] 246-48 (1998).
9. Y. Yosizawa, S. Oguma, and K. Yamaguchi, "New Fe-Based Soft Magnetic Allots Composed of Ultrafine Grain Structure," *J. Appl. Phys.*, **64** [10] 6044-46 (1988).
10. S. Ohnuma, H. Fujimori, S. Mitani, and T. Masumoto, "High-Frequency Magnetic Properties in Metal-Nonmetal Granular Films," *J. Appl. Phys.*, **79** [8] 5130-35 (1996).
11. S. Ohnuma, N. Kobayashi, T. Masumoto, S. Mitani, and H. Fujimori, "Soft Magnetic Properties of Co-Fe-Al-O Thin Films with High B_s," *J. Magn. Soc. Jpn.*, **23** [1-2] 240-42 (1999).
12. S. Ohnuma, N. Kobayashi, T. Masumoto, S. Mitani, and H. Fujimori, "Magnetostriction and Soft Magnetic Properties of $(Co_{1-x}Fe_x)$-Al-O Granular Films with High Electrical Resistivity," *J. Appl. Phys.*, **85** [8] 4574-76 (1999).
13. B. C. Wadell, Transmission Line Design Handbook, Norwood, MA: Artech House, 1991.
14. J. C. Sohn, D. J. Byun, and S. H. Lim, "Nanogranular Co-Fe-Al-O Sputtered Thin Films for Magnetoelastic Device Applications in the GHz Frequency Range," *J. Magn. Mater.*, **272-276** 1500-03 (2004).
15. K. Ikeda, K. Kobayashi, and M. Fujimoto, "Microstructure and Magnetic Properties of (Co-Fe)-Al-O Thin Films," *J. Am. Ceram. Soc.*, **85** [1] 169-73 (2002).
16. M. Fujimoto, N. Narita, H. Takahashi, M. Nakazawa, Y. Kamiyama, and S. Sekiguchi, "Miniaturization of Chip Inductors using Multilayer Technology and Its Application as Chip Components for High-Frequency Power Modules," *Ind. Ceram. (Faenza, Italy)*, **21** [1] 26-8 (2001).
17. H. Fujimori, S. Mitani, T. Ikeda, and S. Ohnuma, "High Electrical Resistivity and Permeability of Soft Magnetic Granular Alloys," *IEEE Trans. Magn.*, **30** 4779-81 (1994).
18. G. Herzer, "Grain Size Dependence of Coercivity and Permeability in Nanocrystalline Ferromagnets," *IEEE Trans. Magn.*, **26** [5] 1397-402 (1990).
19. J. C. Sohn and D. J. Byun, "Prototype Electromagnetic-Noise Filters Incorporated with Nano-Granular $Co_{41}Fe_{38}Al_{13}O_8$ Soft Ferromagnetic Thin Films on Coplanar Transmission Lines(*in Korean*)," *J. Kor. Ceram. Soc.*, **43** [2] 74-8 (2006).